CVS $Revision: 2.2 $Date: 2003/09/11 13:30:28
Preprint typeset using LaTeX style emulateapj v. 7/15/03

DARK ENERGY CONSTRAINTS FROM WEAK LENSING CROSS-CORRELATION COSMOGRAPHY

G. Bernstein & B. Jain
Dept. of Physics and Astronomy, University of Pennsylvania, Philadelphia, PA 19104
accepted to ApJ

ABSTRACT

We present a method to implement the idea of Jain & Taylor (2003) to constrain cosmological parameters with weak gravitational lensing. Photometric redshift information on foreground galaxies is used to produce templates of the mass structure at foreground slices z_ℓ, and the predicted distortion field is cross-correlated with the measured shapes of sources at redshift z_s. The variation of the cross-correlation with z_s depends purely on ratios of angular diameter distances. We propose a formalism for such an analysis that makes use of all foreground-background redshift pairs, and derive the Fisher uncertainties on the dark energy parameters that would result from such a survey. Surveys from the proposed SNAP satellite or the LSST observatory could constrain the dark energy equation of state to $\sigma_{w_0} \approx 0.01 f_{\rm sky}^{-1/2}$ and $\sigma_{w_a} \approx 0.035 f_{\rm sky}^{-1/2}$ after application of a practical prior on Ω_m. Advantages of this method over power-spectrum measurements are that it is unaffected by residual PSF distortions, is not limited by sample-variance, and can use non-linear mass structures to constrain cosmology. The signal is, however, very small, amounting to a change of a few parts in 10^3 of the lensing distortion. In order to realize the full sensitivity to cosmological parameters, the calibration of lensing distortion must be independent of redshift to comparable levels, and photometric redshifts must be similarly free of bias. Both of these tasks require substantial advance over the present state of the art, but we discuss how such accurate calibrations might be achieved using internal consistency tests. Elimination of redshift bias would require spectroscopic redshifts of $\sim 10^4 - 10^5$ high redshift galaxies—fewer for lensing surveys less ambitious than SNAP or LSST.

Subject headings: gravitational lensing; cosmological parameters

1. INTRODUCTION

Weak gravitational lensing is already one of the more accurate constraints on cosmological parameters: several groups have measured the power spectrum of the shear induced on background galaxies by foreground mass fluctuations, leading to $\approx$ 10% constraints on the matter power spectrum normalization σ_8 (Bacon *et al.* 2002; Brown *et al.* 2003; Hamana *et al.* 2002; Hoekstra, Yee, & Gladders 2002; Jarvis *et al.* 2003; Refregier *et al.* 2002; van Waerbeke *et al.* 2002). The weak lensing method has potential for much more precise constraints on σ_8 and other parameter combinations, once larger sky areas are surveyed. The addition of redshift information on the source galaxies allows measurement of the mass power spectrum as a function of redshift, which is expected to greatly increase the accuracy of weak lensing cosmological constraints (Hu 1999, 2002a,b; Huterer 2002; Abazajian & Dodelson 2002; Heavens 2003; Refregier *et al.* 2003; Knox 2003) and permit reconstruction of the three-dimensional mass distribution (Taylor 2001; Hu & Keeton 2002). Weak lensing surveys currently underway such as the CFHT Legacy Survey[1] (CFHLS) and the Deep Lens Survey[2] will gather photometric redshift information to facilitate this "tomographic" analysis.

The successful constraint of the mass power spectrum and cosmological parameters at $\approx 1\%$ levels will require reduction of several sources of systematic error. On the theoretical side, there are not yet predictions of the mass power spectrum $P(k,z)$ that are accurate to the percent level in the non-linear regime (see Linder & Jenkins (2003) for further discussion). A concerted application of N-body computing would likely yield the dark-matter spectrum to desired accuracy, though on very small scales the contribution of baryons to the power spectrum must be included, and will be difficult to calculate. The inaccuracies of power-spectrum estimation may be bypassed by using only large-scale information, where linear or perturbative calculations suffice, but this means discarding most of the lensing information, which lies at non-linear scales.

On the measurement side, currently published power-spectrum measurements all show contamination by systematic errors at the $\approx$ 10% level or higher. This systematic power is likely residual from the process of correcting galaxy shapes for point-spread function (PSF) effects. New methodologies have been introduced (Bernstein & Jarvis 2002; Refregier 2003; Kaiser 2000) which should greatly reduce the systematic contamination, but this remains to be demonstrated. There are also subtle difficulties in calibrating the weak lensing signal to 1% accuracy (Bernstein & Jarvis 2002; Hirata & Seljak 2003).

Jain & Taylor (2003) introduce a new method for analysing weak-lensing data with depth information which promises to largely bypass these systematic difficulties. The basic concept is to use the survey's photometric redshift data to create a map of the foreground galaxies, from which an estimated map of the foreground mass can be made. This foreground mass slice induces shear on all the galaxies in the background. The measurement consists of tracking the amplitude of the in-

Electronic address: garyb, bjain@physics.upenn.edu
[1] www.cfht.hawaii.edu/Science/CFHLS/
[2] dls.bell-labs.com/

duced shear as a function of the background redshift. Once a foreground shear "template" at z_l is created, the dependence of shear on the source redshift z_s is given solely by geometric factors. By taking ratios of induced shears at different z_s, any sensitivity to errors in the foreground mass template is cancelled out, leaving us with a purely geometric observable. One is not attempting to discern the line-of-sight structure, so this is not tomography. We could call this "cross-correlation cosmography" since the measured quantities are metric elements of the homogeneous cosmology.

The idea of using lensing effects on sources at differing redshift to constrain cosmological parameters has been examined before (Link & Pierce 1998; Gautret, Fort, & Mellier 2000; Golse, Kneib, & Soucail 2002; Sereno 2002), with Jain & Taylor offering a methodology for massive datasets that is insensitive to the nature of cluster or halo profiles and examines a time-dependent dark energy component.

The practical advantages of cross-correlation cosmography include:

- No theoretical estimate of the mass power spectrum is required. The mass fluctuations are estimated directly from the foreground galaxy distribution, and any inaccuracies (*e.g.* bias) are cancelled out in the analysis. The observables are hence calculable to arbitrary accuracy.
- With no need for a modelled power spectrum, we can use shear information on all scales sampled by the data. The lensing distortion variance $\langle d^2\rangle$ is $\sim (5\%)^2$, which is at least two orders of magnitude larger than the variance due solely to linear-regime fluctuations. Hence the signal-to-noise ratio (S/N) of the weak lensing data will be much higher.
- Because the background shear is being cross-correlated with a template, the shear signal enters only linearly into the statistics. Systematic power (*e.g.* PSF residuals) average to zero since they will not correlate with the foreground shear template. This makes the PSF-correction task immensely easier than for power-spectrum tomography, in which systematic power adds to the shear power. For cross-correlation cosmography, systematic power may increase uncertainties but does not bias the results. In the language of experimenters, we have changed from a total-power measurement to a phase-sensitive method.
- Uncertainties in calibration of the shear signal also cancel if they are independent of z_s, since we will be interested only in ratios of shear at different z_s. We shall see below, however, that the method is highly sensitive to *differential* calibration errors.

Taking the ratio of shear signals at different z_s provides a pure geometric measurement, but taking this ratio does decrease the dependence of the signal on cosmological parameters. Large numbers of galaxies must be surveyed in order to reduce random errors to make up for the smaller signals, but surveys of up to 10^9 galaxies are currently being planned.

In this paper we investigate the potential of cross-correlation cosmography by proposing an analysis methodolgy that appears close to optimal, and calculating the expected cosmological-parameter uncertainties with the Fisher-matrix method. We then apply this analysis to some planned weak lensing surveys. Finally we return to the issue of systematic errors, exploring the accuracies that will be required for photometric redshift estimates and shear calibration.

2. CROSS-CORRELATION FORMALISM

2.1. *The Observable Quantity*

The underlying assumption of the method is that the observed ellipticity of background galaxy $k \in \{1, 2, \ldots, N\}$ is

$$\mathbf{e}_k^{\rm obs} = \sum_\ell \mathbf{d}_\ell(\mathbf{x}_k) g_{\ell k} + \mathbf{d}_{k,\rm sys} + \mathbf{e}_k, \qquad (1)$$

The quantities of interest will be the geometric factors

$$g_{\ell s} \equiv \frac{r(\chi_s - \chi_\ell)}{r(\chi_s)}, \qquad (2)$$

where χ_ℓ and χ_s are the comoving distances to a lens and source planes, and $r(\chi)$ is comoving angular diameter distance. For a flat Universe, $r(\chi) = \chi$. Each of the $\mathbf{d}_\ell$ is the distortion field[3] imparted on a source plane at $\chi = \infty$ by the mass in redshift shell ℓ. It can be expressed as an integral over the mass distribution in the redshift shell by well-known formulae, *e.g.* Bartelmann & Schneider (2001). Note that the distortion $\mathbf{d}$ is twice the shear $\boldsymbol{\gamma}$ in the weak-lensing limit. Its variance $\langle d_\ell^2\rangle$ can be calculated as an integral of the mass power spectrum $P(k, z_\ell)$, with the formula in Appendix A. Our method, however, will be to make as little use as possible of the power spectrum.

Equation (1) is correct only in the limit that the induced distortion $\mathbf{d}_\ell$, the instrumental systematic distortion $\mathbf{d}_{k,\rm sys}$, and the intrinsic galaxy shape $\mathbf{e}_k$ are all $\ll 1$. The addition operator in distortion space is in fact nonlinear (Bernstein & Jarvis 2002), a detail that will be important, but manageable if we avoid the $\approx 1\%$ of the sky where the lensing distortion is strong.

Any weak lensing measurement maximizes the likelihood of the measured $\mathbf{e}_k^{\rm obs}$ under some model for the shear planes $\mathbf{d}_\ell$ (and perhaps the systematic error contribution simultaneously). In power-spectrum tomography, one varies the assumed power spectra of the $\mathbf{d}_\ell$ to best match the observed covariances of the $\mathbf{e}_k^{\rm obs}$. In our case, we will assume that is possible to produce some estimate $\hat{\mathbf{d}}_\ell$ of the distortion pattern without reference to the background galaxy-shape information. In practice this template distortion would be developed from the galaxies identified near z_ℓ from the photometric redshift data. This could be as simple as convolving the galaxy distribution with an isothermal halo model, or perhaps involve a more sophisticated identification of groups and clusters. We allow that the template distortion is inaccurate to some level, due to galaxy bias or other errors:

$$\langle \mathbf{d}_\ell \cdot \hat{\mathbf{d}}_\ell\rangle = \beta_\ell \langle d_\ell^2\rangle \qquad (3)$$

β_ℓ is a measure of the fidelity of our template, and is related to the bias b and correlation coefficient r between

[3] The distortion denoted as $\boldsymbol{\delta}$ in Bernstein & Jarvis (2002) is labelled $\mathbf{d}$ here in order to avoid confusion with the Kronecker delta.

galaxies and mass, *e.g.* as measured by Hoekstra *et al.* (2002b).

To isolate the geometric term, we correlate the template distortion with the measured distortion. We wish to sum the measurements from all source galaxies in some bin s of redshift centered on z_s. When the shape noise is dominant, the sum which is optimal in the sense of best S/N on $g_{\ell s}$ is

$$X_{\ell s} \equiv \frac{1}{N_s} \sum_{k \in s} \mathbf{e}_k^{\rm obs} \cdot \hat{\mathbf{d}}_\ell(\mathbf{x}_k). \tag{4}$$

Here N_s is the number of source galaxies in bin s. Under the model in Equation (1) the $X_{\ell s}$ will be

$$X_{\ell s} = \sum_{\ell'} R_{\ell\ell'} g_{\ell' s} + \langle \hat{\mathbf{d}}_\ell \cdot \mathbf{d}_{\rm sys} \rangle_s + \langle \hat{\mathbf{d}}_\ell \cdot \mathbf{e} \rangle_s \tag{5}$$

$$R_{\ell\ell'} \equiv \langle \hat{\mathbf{d}}_\ell \cdot \mathbf{d}_{\ell'} \rangle_s \tag{6}$$

Here the subscript s on the average means that we are averaging over the galaxies in source bin s, as in equation 4, not over realizations of the distortion fields. For a given survey, the cosmology predicts the $g_{\ell s}$ values, the templates are known, and the $R_{\ell\ell'}$ are free parameters. The cosmological parameters $\{p_i\}$ are determined by fitting the $\mathbf{X} = \{X_{\ell s}\}$ data vector to the model (5) with free parameters $\{p_i, R_{\ell\ell'}\}$, then marginalizing over the cross-correlations $\{R_{\ell\ell'}\}$ to obtain confidence bounds for the p_i. The intrinsic ellipticities and perhaps systematic errors act as measurement noise on each $X_{\ell s}$.

We now assume that the intrinsic ellipticities $\mathbf{e}_k$ and the systematic-error distortion $\mathbf{d}_{k,\rm sys}$ are independent of the template. We also assume that the distortions and templates are uncorrelated between lens shells, so that $\langle R_{\ell\ell'} \rangle = 0$ for $\ell \neq \ell'$. This last assumption is true if the shells are much thicker than the correlation length of the mass distribution; any correlations could be accommodated in a more sophisticated analysis, or eliminated by applying high-pass filters to the templates. With these assumptions, the expectation value for the $X_{\ell s}$ when we average over realizations of the distortion fields is

$$\langle X_{\ell s} \rangle = \langle R_{\ell\ell} \rangle g_{\ell s} = \beta_\ell \langle d_\ell^2 \rangle g_{\ell s}. \tag{7}$$

2.2. *Covariance Matrix and Likelihood*

In order to calculate probabilities for fits to the $\mathbf{X}$ vector we need its covariance matrix $\mathbf{C}_x$. From the definition (4) and the model (1) we can obtain the covariance in a straightforward manner. Note that when fitting to the model (1) we will be considering only the shape noise and systematic errors to be random variables. The distortion planes, or more precisely the cross-correlations $R_{\ell\ell'}$, are considered as free parameters in the fit, not random variables. We will henceforth ignore the systematic distortion $\mathbf{d}_{\rm sys}$, assuming that it is a minor contributor to the noise compared to the shape noise $\mathbf{e}$. We have already seen that the systematic errors do not bias the observables if they are uncorrelated with the templates.

We assume the $\mathbf{e}_k$ to be independent, with $\mathrm{Var}(e_+) = \mathrm{Var}(e_\times) \equiv \sigma_e^2$ the variance in each component. Intrinsic correlations of galaxy shapes may slightly inflate our uncertainties, but should again be uncorrelated with the $\hat{\mathbf{d}}_\ell$ and hence will not bias the fit. In this case we have

$$(\mathbf{C}_x)_{\ell s \ell' s'} = \mathrm{Cov}(X_{\ell s} X_{\ell' s'}) = \delta_{ss'} \frac{\sigma_e^2}{N_s} \langle \hat{\mathbf{d}}_\ell \cdot \hat{\mathbf{d}}_{\ell'} \rangle_s$$

$$\begin{cases} = \frac{\sigma_e^2 \langle \hat{d}_\ell^2 \rangle}{N_s} & \ell = \ell' \\ \approx 0 & \ell \neq \ell' \end{cases} \tag{8}$$

The $\ell \neq \ell'$ cross-correlation is negligibly small if the survey is much larger than the correlation length of the distortion templates.

The distributions of the $\mathbf{d}_\ell$ and $\mathbf{e}_k$ are very non-Gaussian. For a survey with many source galaxies and an area much larger than the distortion correlation length, however, the distribution for $X_{\ell s}$ should approach Gaussian by the central limit theorem. The likelihood of an observed $\mathbf{X}$ vector given a choice of model parameters is then given by the usual Gaussian formula with covariance matrix $\mathbf{C}_x$. With the likelihood, we may produce confidence bounds on the parameters of the underlying geometry, once we marginalize over the unknown $R_{\ell\ell'}$.

2.3. *Fisher Uncertainties*

Given the likelihood function, the minimal uncertainties on the model parameters may be derived from the Fisher matrix:

$$F_{ij} = -\left\langle \frac{\partial^2 \mathcal{L}}{\partial p_i \partial p_j} \right\rangle \tag{9}$$

where $\mathcal{L} \equiv \log L$. The Fisher matrix for the Gaussian case is well known, *e.g.* Tegmark, Taylor, & Heavens (1997):

$$\mathbf{F}_{ij} = \frac{1}{2} \mathrm{Tr}(\mathbf{C}^{-1} \mathbf{C}_{,i} \mathbf{C}^{-1} \mathbf{C}_{,j}) + \langle \mathbf{X}_{,i}^T \rangle \mathbf{C}^{-1} \langle \mathbf{X}_{,j} \rangle. \tag{10}$$

As usual the subscripts with commas denote derivatives. This simplifies considerably in our case, as $\mathbf{C}_x$ is diagonal and independent of the parameters.

The model parameters are of two kinds: the nuisance parameters $\{R_{\ell\ell'}\}$ and the cosmological parameters $\{p_i\}$. We wish to split the Fisher matrix into submatrices $\mathbf{F}_{RR}$, $\mathbf{F}_{pR}$, and $\mathbf{F}_{pp}$. Henceforth we will adopt the convention that Greek indices (or ℓ) range over the lens planes, the s index runs over source planes, and other Latin indices (except ℓ) range over the cosmological parameters. Keeping in mind that it takes two Greek indices to specify one R component, the three submatrices $\mathbf{F}_{RR}$, $\mathbf{F}_{pR}$, and $\mathbf{F}_{pp}$ are respectively

$$\mathbf{F}_{\alpha\beta\mu\gamma} = \delta_{\alpha\mu} \sum_s \frac{N_s}{\sigma_e^2 \langle \hat{d}_\alpha^2 \rangle} g_{\beta s} g_{\gamma s} \tag{11}$$

$$= \delta_{\alpha\mu} \frac{N}{\sigma_e^2 \langle \hat{d}_\alpha^2 \rangle} \mathbf{G}_{\beta\gamma} \tag{12}$$

$$\mathbf{F}_{i\alpha\beta} = \frac{N}{\sigma_e^2 \langle \hat{d}_\alpha^2 \rangle} \sum_\gamma R_{\alpha\gamma} (\mathbf{G}_i)_{\beta\gamma} \tag{13}$$

$$\mathbf{F}_{ij} = \sum_\alpha \frac{N}{\sigma_e^2 \langle \hat{d}_\alpha^2 \rangle} \sum_{\beta\gamma} R_{\alpha\beta} R_{\alpha\gamma} (\mathbf{G}_{ij})_{\beta\gamma}. \tag{14}$$

The geometric factors are encoded in the matrices

$$(\mathbf{G})_{\alpha\beta} \equiv \int dz_s \frac{dn}{dz_s} g_{\alpha s} g_{\beta s} \tag{15}$$

$$(\mathbf{G}_i)_{\alpha\beta} \equiv \int dz_s \frac{dn}{dz_s} g_{\alpha s} \frac{dg_{\beta s}}{dp_i} \tag{16}$$

$$(\mathbf{G}_{ij})_{\alpha\beta} \equiv \int dz_s \frac{dn}{dz_s} \frac{dg_{\alpha s}}{dp_i} \frac{dg_{\beta s}}{dp_j} \tag{17}$$

The redshift distribution of sources dn/dz is normalized to unit integral, and N is the total number of sources in the survey. There is no loss of information in moving to infinitesimal source-redshift bins.

2.4. *Prior Information*

We are interested in the covariance matrix $\mathbf{C}_p$ of the geometric parameters after marginalization over the R parameters. If L is the number of lens planes in the model, there are L^2 free $R_{\ell\ell'}$ being marginalized, and after this marginalization the constraints on the cosmological parameters are relatively weak for envisioned surveys.

There is, however, additional information about the R values that has not been incorporated into the model of Equation (5), and hence not in the Fisher matrix of Equation (11). We expect that the $R_{\ell\ell'}$ are near zero for $\ell \neq \ell'$ because the lens planes are uncorrelated. We incorporate this knowledge with a prior probability on the R values. If the prior is Gaussian, then we may add the inverse of the R covariance matrix to the $\mathbf{F}_{RR}$ component of the Fisher matrix.

Note that until this point we have had no use for an *ensemble* of mass distributions; all of the quantities in the solution and Fisher matrix for the cosmological parameters make use of just the $R_{\ell\ell'}$ for the single realization of the mass distribution that exists in our survey field. It is only in assembling a prior on these values (and in estimating typical values in §2.5) that we make use of the ensemble properties of the mass distribution. This is why the sample variance contribution is unimportant in the uncertainties of the cross-correlation method.

In the Appendix we show that the covariance matrix for $R_{\ell\ell'}$ is nearly diagonal. The diagonal terms are

$$\mathrm{Cov}(R_{\alpha\beta}R_{\alpha\beta}) = \langle \hat{d}^2_\alpha \rangle \langle d^2_\beta \rangle \frac{\Omega_{\alpha\beta}}{\Omega}. \tag{18}$$

Here Ω is the total solid area of the survey and $\Omega_{\alpha\beta}$ is a measure of the area of coherence of the two distortion fields $\mathbf{d}_\alpha$ and $\mathbf{d}_\beta$. For redshift ranges of interest, $\Omega_{\alpha\beta} \lesssim 1\,\mathrm{arcmin}^2$. The only off-diagonal terms in the covariance matrix for the R values are $\mathrm{Cov}(R_{\alpha\beta}R_{\beta\alpha})$. To simplify the following algebra, we take the covariance matrix for our prior on R to have diagonal elements that are twice as large as Equation (18) and drop the covariance between $R_{\alpha\beta}$ and $R_{\beta\alpha}$. This prior distribution is less restrictive than is the full covariance matrix, so we are at liberty to make this choice.

As a cautionary step we do not make use of the prior information on $R_{\alpha\alpha}$. This is because $R_{\alpha\alpha}$ appears in the expectation value $\langle X_{\alpha s} \rangle$ in Equation (7), and hence prior assumptions may bias the fit for the cosmological parameters that drive the $g_{\alpha s}$ in this fit.

With this simplified, diagonal prior for the R values, the Fisher matrix for the system is altered from Equation (11) as

$$\begin{aligned} \mathbf{F}_{\alpha\beta\mu\gamma} &\to \delta_{\alpha\mu} \frac{N}{\sigma_e^2 \langle \hat{d}^2_\alpha \rangle} \left[\mathbf{G}_{\beta\gamma} + \delta_{\beta\gamma}(1-\delta_{\alpha\beta}) \frac{\sigma_e^2}{2n\Omega_{\alpha\beta}\langle d^2_\beta \rangle} \right] \\ &\equiv \delta_{\alpha\mu} \frac{N}{\sigma_e^2 \langle \hat{d}^2_\alpha \rangle} (\mathbf{G} + \mathbf{P}_\alpha)_{\beta\gamma} \end{aligned} \tag{19}$$

$\mathbf{P}_\alpha$ is simple, having only diagonal elements and a zero at the α element of the diagonal. Here $n = N/\Omega$ is the sky density of source galaxies.

2.5. *Marginalization*

We now return to the marginalization over the $R_{\alpha\beta}$ to obtain a covariance matrix C_p for the cosmological parameters. Using a common matrix identity, we obtain

$$(\mathbf{C}_p^{-1})_{ij} = \left(\mathbf{F}_{pp} - \mathbf{F}_{pR}\mathbf{F}_{RR}^{-1}\mathbf{F}_{pR}^T\right)_{ij} = \frac{N}{\sigma_e^2} \sum_\alpha \frac{1}{\langle \hat{d}^2_\alpha \rangle} \sum_{\beta\gamma} R_{\alpha\beta}R_{\alpha\gamma} \left(\mathbf{G}_{ij} - \mathbf{G}_i^T(\mathbf{G}+\mathbf{P}_\alpha)^{-1}\mathbf{G}_j\right)_{\beta\gamma}. \tag{20}$$

This gives the Fisher uncertainties on cosmological parameters for a survey over a sky with given distortion field and hence given R values. We next average over realizations of the mass distribution in the Universe, which requires that we calculate

$$\langle R_{\alpha\beta}R_{\alpha\gamma} \rangle = \mathrm{Cov}(R_{\alpha\beta}R_{\alpha\gamma}) + \langle R_{\alpha\beta} \rangle \langle R_{\alpha\gamma} \rangle \equiv \delta_{\beta\gamma} \left[\langle \hat{d}^2_\alpha \rangle \langle d^2_\beta \rangle \frac{\Omega_{\alpha\beta}}{\Omega} + \delta_{\alpha\beta} \langle R_{\alpha\alpha} \rangle^2 \right]. \tag{21}$$

Combining Equations (7), (20), and (21), we obtain the expected (inverse) covariance matrix for the cosmological parameters:

$$(\mathbf{C}_p^{-1})_{ij} = \frac{N}{\sigma_e^2} \sum_\alpha \left[\beta_\alpha^2 \langle \hat{d}^2_\alpha \rangle \left(\mathbf{G}_{ij} - \mathbf{G}_i^T(\mathbf{G}+\mathbf{P}_\alpha)^{-1}\mathbf{G}_j\right)_{\alpha\alpha} + \sum_\beta \langle d^2_\beta \rangle \frac{\Omega_{\alpha\beta}}{\Omega} \left(\mathbf{G}_{ij} - \mathbf{G}_i^T(\mathbf{G}+\mathbf{P}_\alpha)^{-1}\mathbf{G}_j\right)_{\beta\beta} \right] \tag{22}$$

We note first that there is no "sample variance limit" to the cross-correlation cosmography measure of the cosmological parameters—uncertainties scale as $1/\sqrt{N}$ as the density of sources becomes large. Sample variance typically arises when one does not measure enough independent patches of the density field to adequately constrain its power spectrum. In our application, however, we are not using the power spectrum to measure cosmology, we

instead are just cross-correlating the observations with whatever mass distribution the Universe gives us. Hence there is no sample variance contribution.

The left-hand term in Equation (22) arises purely from the shape noise in the measured field that is being cross-correlated with the templates, while the right-hand term arises because the distortion from one lens slice acts as a correlated noise source for all the $X_{\ell s}$. The right-hand term has an amplitude $\approx L/N_c$ relative to the left-hand term, where L is the number of lens planes and $N_c = \Omega/\Omega_{\alpha\beta}$ is the number of independent cells or patches of the distortion fields. In almost any large survey we should be able to choose the lens-plane width Δz_ℓ to be sufficiently narrow that the $g_{\ell s}$ do not vary significantly within the bin, and still have $L/N_c \ll 1$. In other words we will usually have more than enough independent patches to decorrelate the different lens planes.

In the regime where the left-hand term dominates, the parameter accuracy is essentially independent of the foreground binning, as long as the fidelity β_ℓ remains high and the shells remain uncorrelated.

3. APPLICATION TO CANDIDATE SURVEYS

3.1. *Cosmological Parameters*

Any parameter that influences growth factor $a(t)$ or curvature of the Universe will have some effect on the $\mathbf{X}$ data via $g_{\ell s}$; in particular we will be interested in the present-day matter and energy densities Ω_m and Ω_X, and the parameters w_0 and w_a that approximate the equation of state of the dark energy via (Linder 2003)

$$P_X = [w_0 + w_a(1-a)]\rho_X. \tag{23}$$

We will henceforth assume a flat Universe $\Omega_X = 1-\Omega_m$, in which case we have (Linder 2003)

$$r[\chi(z)] = \chi(z) = \frac{c}{H_0}\int_0^z dz' \left[\Omega_m(1+z')^3 + (1-\Omega_m)(1+z')^{3(1+w_0+w_a)}e^{-3w_a z'/(1+z')}\right]^{-1/2}$$

Unless otherwise noted, we will calculate the sensitivity to departures from the canonical ΛCDM model ($\Omega_m = 0.3, w_0 = -1, w_a = 0$).

3.2. *Mass Variance*

The distortion power generated by a mass slice at z_l and the coherence areas $\Omega_{\alpha\beta}$ can be estimated by applying the formulae in the Appendix to a model for the non-linear evolution of the power spectrum. We reiterate that errors in this model will affect only our forecasted uncertainty, not the derived cosmological parameters.

We use the nonlinear mass power spectrum given by the fitting formula of Peacock & Dodds (1996), with implementation for weak lensing as described in Jain & Seljak (1997). We need this only for the fiducial ΛCDM model, for which the differences between different fits to N-body simulations are small (Smith *et al.* 2002). The integrals over the power spectrum are cut off for $k > 2\pi/(50\,\mathrm{kpc})$; this is a crude way of accounting for the fact that we will have to exclude the central regions of galaxy clusters, where the lensing is strong and where the light of the foreground galaxies may preclude observation of the background galaxies. The results are not sensitive to the choice of the high-k cutoff. We will assume that the estimated templates $\hat{\mathbf{d}}_\ell$ have the same variance as the true distortion fields $\mathbf{d}$, but with fidelity $\beta_\ell = 0.8$. The uncertainties on cosmological parameters will scale as β_ℓ^{-1}.

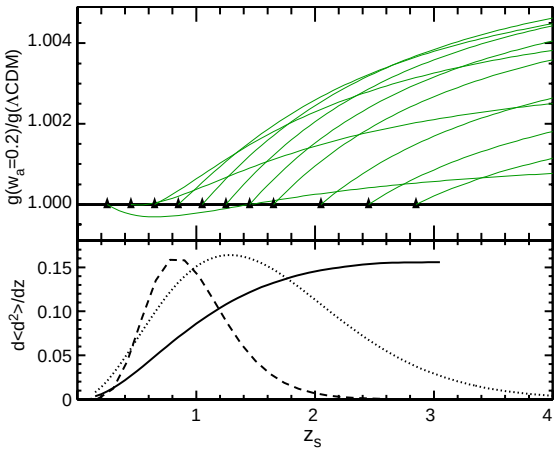

FIG. 1.— The top panel shows the fractional change in the geometric factor $g_{\ell s} = (\chi_s - \chi_\ell)/\chi_s$ when we shift from a pure ΛCDM Universe to one with $w_a = 0.2$; this should be discernible at 1σ significance in the SNAP survey. The horizontal axis is z_s and each line corresponds to a different z_ℓ. The triangle at the end of each line marks z_ℓ. Because the mass normalization in each lens slice is free to vary, vertical shifts of each line carry no cosmological information, so we align them all to be unity at z_ℓ. The cosmological information is carried in the departures of each line from horizontal; these departures are small, amounting to only a few parts in 10^{-3} change in the induced background distortion. The smallness of this signal implies that the calibration of the distortion measurement and the source redshifts must be accurate to roughly a part in 10^3. The lower panel plots the assumed source redshift distribution (dotted line) and the expected distortion variance per unit redshift (solid line) using estimated non-linear power spectra. The dashed line shows the relative contribution of different lens planes to the constraint on w_a.

The bottom panel of Figure 1 plots the strength of lensing distortion vs redshift, $d\langle d^2\rangle/dz$ that arises from this model. For the coherence angle we use

$$\Omega_{\alpha\beta} = (0.24\,\mathrm{arcmin})^2(\chi_\alpha\chi_\beta)^{-0.8}, \tag{24}$$

which is within $\sim 25\%$ of the more carefully calculated values. The coherence area has only a minor impact on the cosmological uncertainties.

3.3. *Redshift Distribution*

We adopt the common guess for the redshift distribution of faint galaxies,

$$\frac{dn}{dz} \propto z^2 \exp\left[-(z/z_0)^{1.5}\right], \tag{25}$$

and will select z_0 and the overall density n to crudely mimic the expectations of several future surveys.

3.4. *Parameter Forecasts*

Table 1 lists crudely approximated parameters for three possible weak-lensing surveys: the CFHT Legacy Survey, just beginning and expected to take 5 years to

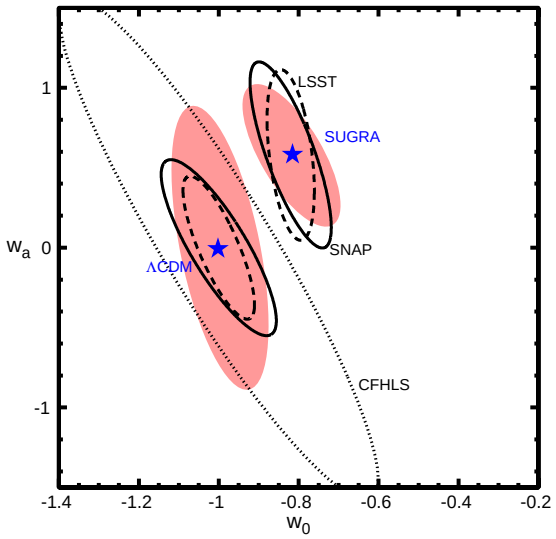

FIG. 2.— Fisher uncertainty ellipses for dark energy parameters derived from three candidate weak lensing surveys are plotted. All ellipses are 68% confidence two-dimensional regions ($\Delta\chi^2 = 2.3$) after application of a Gaussian prior on Ω_m with $\sigma = 0.03$ and marginalization over Ω_m. The solid, dashed, and dotted contours are for SNAP, LSST, and CFHLS surveys, respectively. Survey parameters are listed in Table 1 and a flat Universe is assumed. Fiducial models for both ΛCDM and a supergravity-inspired model are plotted as stars, and the shaded regions are the expected constraints from the SNAP Type Ia supernova measurement plus Ω_m prior (E. Linder, private communication). Unlike the weak lensing contours, the SN contours include the estimated effects of the dominant systematic errors.

cover $\approx 200\,\mathrm{deg}^2$ of sky; a possible deep multicolor lensing survey covering $\sim 10\%$ of the sky with the proposed Large Synoptic Survey Telescope (LSST)[4], and a 400 deg^2 weak lensing survey with the proposed Supernova Acceleration Probe (SNAP)[5]. The orbiting SNAP focal plane should obtain significantly higher source galaxy densities than the ground-based observatories, with consequently deeper median redshift.

In evaluating the Fisher matrix, we assume that $\sigma_e = 0.3$ and that $\beta_\ell = 0.8$. Cosmological parameter uncertainties will scales as σ_e/β. We use $\Delta z_\ell = 0.2$ for the thickness of the lens slices. This choice has very little impact upon the parameter constraints because the first term dominates Equation (22), *e.g.* changing to $\Delta z_\ell = 0.1$ for the SNAP case alters the parameter constraints by $\lesssim 1\%$.

For each candidate survey we evaluate the cosmological-parameter covariance matrix $\mathbf{C}_p$ using Equation (22). The resultant matrix is highly degenerate in one direction, so we adopt a Gaussian prior distribution on Ω_m with $\sigma = 0.03$. The constraints in the $w_0 - w_a$ plane after applying this prior and marginalizing over Ω_m are plotted in Figure 2 for the three surveys. Table 1 also lists the 1-σ uncertainties in w_0 and w_a (assuming in each case marginalization over all other parameters) and the correlation coefficient between these two parameters.

For both the SNAP and LSST surveys, the constraints on the dark energy equation of state and its evolution are quite strong, comparable to or tighter than those of any proposed experiment of which we are aware. The 1-σ uncertainties on w_a, even after marginalizing over all other parameters, are $\sigma_{w_a} \approx 0.3$ in both cases. In terms of the commonly used parameter $w' \equiv [dw/d\ln(1+z)]_{z=1} = w_a/2$ we have $\sigma_{w'} \approx 0.15$.

3.5. *Dependence of Constraints on Survey Parameters*

The Fisher uncertainties from the weak lensing survey will scale as $f_{\rm sky}^{-1/2}$. Because the prior on Ω_m is independent of f_{sky}, the marginalized error ellipses do not quite scale as $f_{\rm sky}^{-1/2}$, but this is a valid approximation in the neighborhood of the canonical survey parameters.

Increased survey depth leads to both greater source density n and greater median redshift $z_{\rm med}$. Parameter uncertainties scale as $n^{-1/2}$ (again not quite because of the prior), and hence unlike power-spectrum tomography, there is no breakpoint at which cosmic variance limits a survey of a given size. The additional depth is also a benefit: changing $z_{\rm med}$ from 1.0 to 1.5 decreases the error on w_a by 23%, if the galaxy density and survey area are held fixed. In other words, the increased depth makes each galaxy about 1.5 times more valuable.

The lower panel of Figure 1 illustrates the contribution of different lens planes to the constraint on w_a for the SNAP survey. Most of the information comes from lens planes near $z = 1$, but if a deeper source distribution were available, lens planes at higher z would continue to add significant information. It would be particularly interesting to see how this behavior is altered with inclusion of the cosmic microwave background as a source screen at $z \simeq 1000$.

Combining these various scalings, the overall constraint on evolution of the dark energy equation of state will scale roughly as

$$\sigma_{w_a} \propto \left(\frac{\sigma_e^2}{n f_{\rm sky}\beta^2}\right)^{0.5} z_{\rm med}^{-0.6} \qquad (26)$$

3.6. *Comparison with Jain & Taylor*

Our parameter constraints can be compared with those obtained by Jain & Taylor (2003) who used a simplified implementation of the cross-correlation approach. The measurement suggested by them was the tangential shear around foreground halos, identified using galaxy groups and clusters. They assumed that essentially all halos out to $z = 1$ with mass $> 4 \times 10^{13} M_\odot$ could be identified this way. For a given lens slice they used source galaxy shapes on only $\simeq 10\%$ of the sky. This approach corresponds to taking a particularly simple construction of the template shear map. Other simplifications made by Jain & Taylor were that intrinsic ellipticity shot noise was taken to be the only source of error and only two bins in source redshift were used for each lens slice. We find that the method presented here can improve parameter constraints, primarily due to the use of more than two redshift slices. However our results for σ_w and σ_{w_a} are close to those of Jain & Taylor because the size of the single-parameter marginalized errors is, for the large surveys considered, controlled by the prior for Ω_m.

[4] www.dmtelescope.org/dark_home.html
[5] snap.lbl.gov

Table 1. Future Weak Lensing Surveys and Dark Energy Constraints

Survey	Median z	Galaxy Density (arcmin^{-2})	$f_{\rm sky}$	w_0 Error	w_a Error	$w_0 - w_a$ Correlation
CFHLS	1.0	30	0.005	0.26	1.04	-0.92
LSST	1.0	30	0.1	0.06	0.30	-0.80
SNAP	1.5	100	0.01	0.10	0.36	-0.83

4. SYSTEMATIC ERRORS

The cross-correlation cosmography technique is essentially insensitive to several of the largest systematic error sources in power-spectrum tomography, namely residual PSF distortion and errors in calculation of the non-linear power spectrum. The technique does, however, place stringent demands on the distortion calibration and photometric redshift accuracy of the weak lensing survey. This is illustrated in Figure 1. The top panel plots the fractional change in $g_{\ell s}$ when we move from a ΛCDM universe to one with $w_a = 0.2$. According to the Fisher calculation, this should be detectable at 1σ significance in the SNAP survey.

4.1. *Demands on Distortion Calibration*

Each line in the plot shows $g_{\ell s}$ vs z_s for one choice of z_l. The "signal" in the cross-correlation cosmography method is the departure of these curves from horizontal lines. A pure vertical shift of any line will be degenerate with a change in the fidelity β_ℓ of the template in lens shell ℓ, hence the cosmological information is in the slope/curvature of these lines. We see that the minimum detectable cosmological signature corresponds to a change of ≈ 2 parts in 10^3 of g, and hence an equivalent change in the measured distortion vs z_s. We may immediately conclude that *exploitation of this technique to constrain w_a requires that the distortion calibration be constant to 1 part in* 10^3 *over all measured redshifts.* This will be a significant technical challenge. Hirata & Seljak (2003) demonstrate that present algorithms have calibration errors of 1–10%, so at least an order-of-magnitude improvement is required. Hirata & Seljak (2003) and Bernstein & Jarvis (2002) propose methods to improve calibration accuracy, but these have not yet been demonstrated on real data. Furthermore, most methodologies assume that the distortion is weak, *i.e.* they ignore induced changes to galaxy shape that are of order d^2 or higher. The non-linear effects of even "weak" distortions will have to be accounted for to second or even third order to reach the calibration accuracy of 10^{-3}. Regions where the lensing is strong will clearly have to be avoided.

To estimate the demands of this requirement on the data reduction methodology, we note that the conversion of observed ellipticities to pre-seeing elliptiticities typically involves the factor $(1 + r_\star^2/r^2)$, where r is the angular radius of the (pre-seeing) galaxy and $r_\star$ is the PSF radius. A good weak lensing methodology makes use of galaxies as small as $r \approx r_\star$; in this case, both r and $r_\star$ must be known to better than 1 part in 10^3 in order to obtain a distortion calibration accurate to 1 part in 10^{-3}. If r were independent of z, then we would have redshift-independent calibration errors, which do not affect the cross-correlation method. But fainter, more distant galaxies are typically smaller in angular diameter, so errors in $r_\star$ will couple to the cosmography measurement.

4.2. *Demands on Redshift Determinations*

Our formalism can be adapted to deal with the *random errors* in photometric redshift measurements, but it will still be crucial to minimize *biases* in the photo-z estimates. The quantity $g_{\ell s}$ scales slightly less than linearly with the redshifts z_s and z_ℓ. It is therefore clear that mis-estimates of the mean photometric redshift of a few parts in 10^3 would overwhelm the signal of a $w_a = 0.2$ cosmology. Hence *photometric redshifts must be accurate to* $\approx 10^{-3}$ *in* $\log(1+z)$. This again is at least one order of magnitude beyond the present state of the art.

It is important to realize first that this is not the requirement on the accuracy of *each* measured photometric redshift, but rather a requirement on the *bias* of a collection of photometric redshift estimates. Second, we are not required to use all the galaxies in the image. One would likely choose to exclude from the analysis galaxies whose colors make assignment of a photometric redshift particularly uncertain or ambiguous.

4.3. *Practical Issues*

If the required accuracy of distortion and redshift calibration cannot be achieved, one could introduce additional free parameters in the model to represent calibration errors. These terms would be purely functions of z_s, and hence in theory distinguishable from the cosmological signals, which couple z_ℓ and z_s through $g_{\ell s}$. The constraints on dark energy would be degraded, to an extent that is calculable with further Fisher analysis.

We note that if the random error in a typical photometric redshift is $\sigma_z \approx 0.03(1+z)$, then it will take a spectroscopic survey of $\approx 10^3$ galaxies in order to check that the mean error (bias) is below $10^{-3}(1+z)$. Repeating this bias check in bins of redshift from 0–3 would thus require a sample of 10^4 or 10^5 spectroscopic redshifts to compare with the photometric redshifts. Redshift surveys of this size to limiting magnitudes of 24 or 25 will be feasible: indeed the DEEP2 survey[6] is already well on its way to its goal of 65,000 spectra to $I_{AB} < 24.5$.

Given the extreme demands that cross-correlation cosmography will place on the calibration of both the lensing distortion and photo-z calibrations, there will be a significant advantage to space-based observations. Ground-based analyses must deal with a constantly-varying PSF and atmospheric transmission function which will make it more difficult to achieve these accurate calibrations. A space-based platform will have the additional advantages of thermal stability, a much sharper PSF, and the possibility of using near-IR filter bands to improve the photo-z accuracy.

[6] http://deep.berkeley.edu

5. CONCLUSION

We have presented a formalism for implementing the idea of Jain & Taylor (2003) to constrain cosmology by tracing the dependence of induced distortion on background redshift for a fixed foreground mass template. Cross-correlating the background distortion with a series of foreground mass templates has significant advantages over power-spectrum tomography, particularly its immunity to spurious distortion signals, and the ability to use non-linear lensing structures without having to model accurately the non-linear evolution of matter in the Universe. We believe this formalism makes use of all the information available in all lens-source pairs in a nearly optimal fashion; we find that a survey with median redshift ≈ 1.5 and 100 galaxies per square arcminute can constrain the dark energy parameters to $\sigma_{w_0} \approx 0.01 f_{\rm sky}^{-1/2}$ and $\sigma_{w_a} \approx 0.035 f_{\rm sky}^{-1/2}$ after application of a practical prior on Ω_m.

Realization of the full potential of the cross-correlation cosmography method will require that techniques for the calibration of lensing distortion and photometric redshift be improved by at least an order of magnitude from present state of the art. There are no known fundamental barriers to this, but it will not be easy. We discuss ways of fitting for parameters in the calibration from the data. To reduce possible biases in the photometric redshifts to an acceptable level would require spectroscopic redshifts for $10^4 - 10^5$ galaxies over the redshift range used in the analysis. An orbiting observatory may be preferred for obtaining the precision required for our method due to its greater photometric and optical stability, and access to the near infrared.

The potential accuracy of cross-correlation cosmography on the equation-of-state time variation compares well to the expected precision of power-spectrum tomography. A formalism for full utilisation of the power-spectrum tomography information has not yet been published, and none of the few published investigations of the effects of time-dependent dark energy use Equation (23) for the equation of state. The assumed priors and confidence levels of published estimates also vary greatly, so only crude comparisons can be made. Hu (2002b) estimates an error of $\approx 0.05 f_{\rm sky}^{-1/2}$ on w' from tomography confined to the linear regime. The plots of Benabed & van Waerbeke (2003) suggest $\approx 0.03 f_{\rm sky}^{-1/2}$ from a non-tomographic analysis deep into the non-linear regime. It should ultimately be possible to use all the information encoded in the weak lensing—cosmography, growth function, and cross-correlation with foreground structures—to provide constraints stronger than those we forecast here. By cancelling the growth information, however, we eliminate the systematic errors that might arise from mis-calculation of the theoretical non-linear spectrum, and from *additive* contamination of the distortion field by systematic effects. The penalty for cancelling the growth factor is that the signal is partially cancelled as well, leaving the cross-correlation method more susceptible to *multiplicative, redshift-dependent* errors in the distortion field that might arise from PSF effects.

Further improvements to the cross-correlation cosmography methodology are worth investigation. The cosmic microwave background can serve as an additional source plane at $z_s = 1000$, and its shear pattern can be cross-correlated with all the lens planes to provide a S/N improvement and greater redshift leverage. One could also make use of magnification information as well as shear in the background galaxy samples, which would improve the S/N and serve as a useful cross-check (*e.g.* Jain (2002)). Finally, in this study we have not developed a detailed method to obtain template distortion maps from the foreground galaxy distribution. A detailed study that includes the redshift dependence of the fidelity of the template would be useful.

GMB is supported in this work by grant AST-9624592 from the National Science Foundation. BJ acknowledges the Aspen Center for Physics where part of this work was done and support from NASA grant NAG5-10923. We thank Wayne Hu, Andy Taylor, Jun Zhang, Masahiro Takada and Michael Jarvis for helpful conversations.

REFERENCES

Abazajian, K. & Dodelson, S. 2003, Phys. Rev. Lett., 91, 41301
Bacon, D., Massey, R., Refregier, A., Ellis, R., 2002, astro-ph/0203134
Bartelmann, M., Schneider, P., 2001, Phys. Rep., 340, 291
Benabed, K., & van Waerbeke, L., 2003, astro-ph/0306033
Bernstein, G. & Jarvis, M., 2002, AJ, 123, 583
Brown, M. L., Taylor, A. N., Bacon, D. J., Gray, M. E., Dye, S., Meisenheimer, K., & Wolf, C. 2003, MNRAS, 341, 100
Gautret, L., Fort, B., & Mellier, Y. 2000, A&A, 353, 10
Golse, G., Kneib, J.-P., & Soucail, G. 2002, A&A, 387, 788
Hamana, T., *et al.*, 2002, astro-ph/0210450
Heavens, A. 2003, MNRAS, 343, 1327
Hirata, C. & Seljak, U. 2003, MNRAS, 343, 459
Hoekstra, H., Yee, H. K. C., & Gladders, M. D., 2002, ApJ, 577, 595
Hoekstra, H., van Waerbeke, L., Gladders, M., Mellier, Y., & Yee, H. K. C., 2002b, ApJ, 577, 604
Hu, W., 1999, ApJ, 522, 21
Hu, W., 2002a, Phys. Rev. D, 65, 023003
Hu, W., 2002b, Phys. Rev. D, 66, 083515
Hu, W, Keeton, C.R, 2002, Phys. Rev. D, 66, 063506
Huterer, D, 2002, Phys. Rev. D, 65, 063001
Jain, B., 2000, ApJL, 580, 3
Jain, B. & Seljak, U., 1997, ApJ, 484, 560
Jain, B. & Taylor, A., 2003, astro-ph/0306046
Jarvis, M., Bernstein, G., Jain, B., Fischer, P., Smith, D., Tyson, J. A., Wittman, D., 2003, AJ, 125, 1014
Kaiser, N., 2000, ApJ, 537, 555
Knox, L., 2003, astro-ph/0304370
Linder, E.V., 2003, Phys. Rev. Lett., 90, 091301
Linder, E. & Jenkins, A., 2003, astro-ph/0305286
Link, R. & Pierce, M. J. 1998, ApJ, 502, 63
Peacock, J. A. & Dodds, S. J., 1996, MNRAS, 280, L19
Refregier, A., Rhodes, J., & Groth, E. J., 2002, ApJ, 572, L131
Refregier, A. *et al.*, 2003, astro-ph/0304419
Refregier, A., 2003, MNRAS, 338, 35
Schneider, P., van Waerbeke, L., & Mellier, T., 2002, A&A, 389, 279
Sereno, M. 2002, A&A, 393, 757
Smith, R. E., *et al.*, 2003, MNRAS, 341, 1311
Taylor, A. N., 2001, astro-ph/0111605
Tegmark, M., Taylor, A., Heavens, A., 1997, ApJ, 480, 22
van Waerbeke, L., Mellier, Y., Pelló, R., Pen, U.-L., McCracken, H. J., & Jain, B., 2002, A&A, 393, 369

APPENDIX

COVARIANCE MATRIX OF $R_{\alpha\beta}$

At several points in the analysis we require the covariances of the slice-to-slice distortion correlations $R_{\alpha\beta} \equiv \langle \hat{\mathbf{d}}_\alpha \cdot \mathbf{d}_\beta \rangle$. Under the assumption that $\mathbf{d}_\beta$ is completely uncorrelated with both $\mathbf{d}_\alpha$ and $\hat{\mathbf{d}}_\alpha$, it is clear that the only non-vanishing elements of the covariance matrix are of the form $\mathrm{Var}(R_{\alpha\alpha})$, $\mathrm{Var}(R_{\alpha\beta})$, and $\mathrm{Cov}(R_{\alpha\beta}R_{\beta\alpha})$. We first calculate $\mathrm{Var}(R_{\alpha\beta})$ for $\alpha \neq \beta$:

$$\langle R_{\alpha\beta}R_{\alpha\beta}\rangle = \frac{1}{\Omega^2}\int\int d^2r\, d^2r' \left\langle [\hat{\mathbf{d}}_\alpha(\mathbf{r})\cdot\mathbf{d}_\beta(\mathbf{r})][\hat{\mathbf{d}}_\alpha(\mathbf{r}')\cdot\mathbf{d}_\beta(\mathbf{r}')]\right\rangle \tag{A1}$$

$$= \frac{2}{\Omega}\int d^2r\,[\xi_{\alpha+}(r)\xi_{\beta+}(r) + \xi_{\alpha-}(r)\xi_{\beta-}(r)] \tag{A2}$$

$$= \frac{2}{\Omega}\int \frac{d^2\ell}{(2\pi)^2} P_\alpha(\ell)P_\beta(\ell). \tag{A3}$$

Ω is the solid angle of the survey, and $P_\alpha(\ell)$ and $P_\beta(\ell)$ are the power spectra of the lensing convergence corresponding to the distortion fields $\hat{\mathbf{d}}_\alpha$ and $\mathbf{d}_\beta$, respectively, at spherical harmonic ℓ. We have made use of the shear correlation functions $\xi_\pm$ as defined for example in Schneider, van Waerbeke, & Mellier (2002), who also give these correlation functions in terms of the convergence power spectrum. We may also put the distortion variance in terms of the convergence power spectrum:

$$\langle d_\beta^2\rangle = \frac{4}{(2\pi)^2}\int d^2\ell P_\beta(\ell). \tag{A4}$$

We can now express the covariance straightforwardly as

$$\langle R_{\alpha\beta}R_{\alpha\beta}\rangle = \langle \hat{d}_\alpha^2\rangle\langle d_\beta^2\rangle\frac{\Omega_{\alpha\beta}}{\Omega} \tag{A5}$$

$$\Omega_{\alpha\beta} = \frac{\pi^2}{2}\frac{\int d^2\ell\, P_\alpha(\ell)P_\beta(\ell)}{\int d^2\ell\, P_\alpha(\ell)\int d^2\ell\, P_\beta(\ell)}. \tag{A6}$$

The quantity $\Omega_{\alpha\beta}$ gives the solid angle over which the two distortion fields maintain mutual coherence. We will make the approximation that the template field $\hat{\mathbf{d}}_\alpha$ has a power spectrum with the same shape as the actual field $\mathbf{d}_\alpha$, so that $\Omega_{\alpha\beta}$ has the same value regardless of whether we are correlating the templates or the real distortion, *e.g.*$\Omega_{\beta\alpha} = \Omega_{\alpha\beta}$.

If the lens shell thickness $\Delta\chi$ satisfies $\Delta\chi \ll \chi_\ell$, then we have a simple relation between the convergence power spectrum and the spectrum P_{3d} of mass fluctuations in three dimensions:

$$P_\beta(\ell) = \frac{9H_0^2\Omega_m^2}{4a^2(\chi_\beta)c^4}P_{3d}\left(\frac{\ell}{\chi_\beta},\chi_\beta\right)\Delta\chi \tag{A7}$$

$\mathrm{Cov}(R_{\alpha\beta}R_{\beta\alpha})$ is also non-vanishing; it differs from $\mathrm{Var}(R_{\alpha\beta})$ in that cross-correlations between $\hat{\mathbf{d}}_\alpha$ and $\mathbf{d}_\alpha$ are required. If the template is well correlated with the actual mass then we expect Equation (A5) to describe the covariance up to a factor near unity, *i.e.* $R_{\alpha\beta}$ will be highly correlated with $R_{\beta\alpha}$. We do not need this expression in detail.

The final non-vanishing term is (again ignoring the distinction between template and actual distortion)

$$\mathrm{Var}(R_{\alpha\alpha}) = \frac{1}{\Omega}\int d^2r\,\left\langle \left[d_\alpha^2(0) - \langle d^2\rangle\right]\left[d_\alpha^2(\mathbf{r}) - \langle d^2\rangle\right]\right\rangle, \tag{A8}$$

which clearly involves the four-point correlation functions of the shear field, and hence depends upon the degree of non-Gaussianity in the mass distribution. Equation (A5) will be correct up to a factor of order unity, which we could absorb into the definition of $\Omega_{\alpha\alpha}$. This term does not significantly affect the Fisher matrix.